13th World Conference on Earthquake Engineering
Vancouver, B.C., Canada
August 1-6, 2004
Paper No. 2693

STUDY ON SEMI-ACTIVE ISOLATION SYSTEM WITH MAGNETO-RHEOLOGICAL FLUID DAMPER

Namihiko INOUE[1], Hidekazu NISHIMURA[2], Naoe IWATA[2], Yuu MIYAHARA[2], Jun NAKASONE[3], Morimasa WATAKABE[4], Shigemitsu TAKAI[5], Yoshiya NAKAMURA[6], Takeyoshi FUJINAMI[7] and Hiroaki RYUJIN[7]

SUMMARY

To improve a performance of conventional base isolation system, a semi-active MR damper (kind of oil damper filled with "Magneto-Rheological fluid") that can change damping coefficient continuously under magnetic field has been installed into isolation layer. This semi-active base isolated control system is classified into a bilinear system, which an input of the system is proportional to both one of the state vectors and damping factor. To apply a linear control theory like LQR directly, the system has been formed into an equivalent linear system at a certain condition. Since there is some possibility of deterioration of structural performance that is not desirable from the viewpoint of a reduction of acceleration response, we apply the gain-scheduled (GS) control method by transforming the system with the semi-active MR damper to a parameter variation system and finally demonstrate the efficiency of the method successfully.

INTRODUCTION

In recent years, there have been many efforts to improve performance of base isolated structures against seismic action. Efficacy of a passive isolated system is well known and the base isolation system consisting of some commercial devices such as LRBs, oil dampers etc. has been applied to many buildings in Japan. Since the passive system is tuned to have specified dynamic property, there are some uncertainties about response under future large earthquakes. To avoid this problem, we take semi-active control that may be more stable and reliable than active control. In this paper we use an MR damper that has same specifications as previously developed one [1][2], which can make damping forces appropriate by input current control. In order to obtain control force we apply a "gain-scheduled" control method. In this method the controller have been calculated appropriately through convex interpolation of some linear time invariant controllers according to certain dynamical systems at vertexes of varying parameters. To apply the GS control, a semi-active damper model with controllable valve is assumed and the system is described as a linear parameter-varying (LPV) model.

[1] Dept. of Structural Eng., Building Research Institute, Ibaraki, Japan Email: inoue_n@kenken.go.jp
[2] Faculty of Eng., Chiba Univ., Chiba, Japan [3] Kumagaigumi Co., Ltd., Japan [4] Toda Corp., Japan
[5] Nishimatsu Construction Co., Ltd., Japan [6] Fujita Corp., Japan [7] Maeda Corp., Japan

SYSTEM PARAMETERS

SPECIMEN

Numerical Model

The experimental setup and numerical model used in this paper are shown in Figure 1. The specimen has two stories and is settled on a four meters squared, 1-D shaking table in Structural Laboratory of the Building Research Institute that produces an input ground motion by a hydraulic actuator. There are four rubber bearings and four sliding isolators between the shaking table and the first story, and two rubber bearings and two sliding isolators for the second story. To determine the system parameters of this 2DOF system, free vibration tests has been carried out before installing the MR damper. While isolators have been used to avoid twisting motion of masses, some additional friction forces between each story are observed. See Table 1 for detail.

Frequency responses

Figure 2 shows the frequency responses of each story acceleration to the ground acceleration for the numerical model of structure. The first mode is at 0.36Hz (2.8sec) and the second mode is at 1.07Hz (0.94sec) respectively.

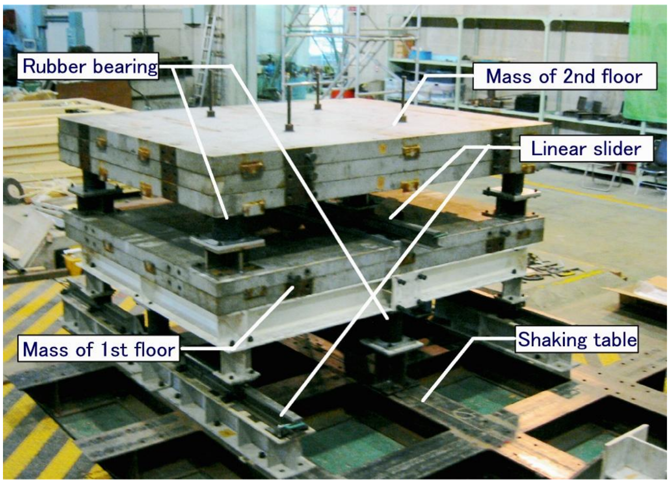

(a) Experimental setup

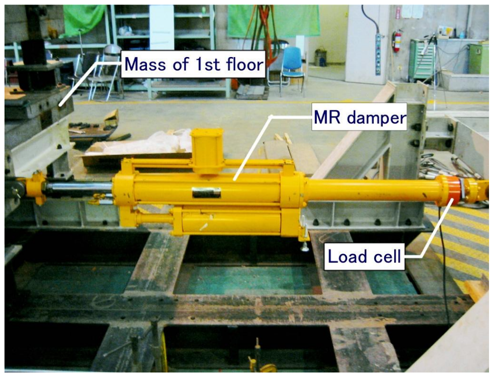

(b) Installation of MR damper

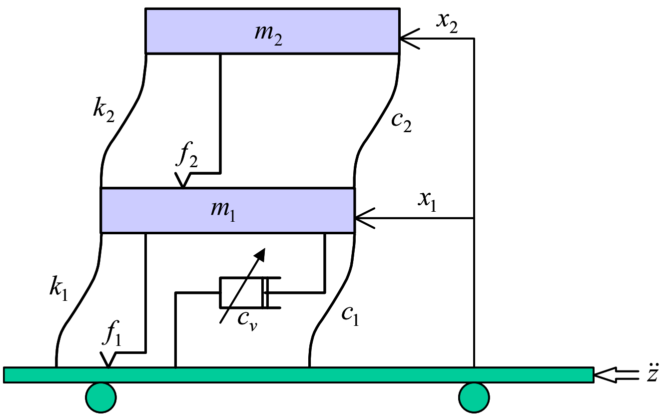

(c) Numerical model

Figure 1. Experimental Setup and Numerical Model of Specimen

Table 1. System Parameters

Parameter		Value
Mass	m_1	5 655.1 [kg]
	m_2	8 770.4 [kg]
Stiffness	k_1	110 880 [N/m]
	k_2	104 950 [N/m]
Damping	c_1	4 527.1 [N s/m]
	c_2	3 591.9 [N s/m]
Friction Force	f_1	471.2 [N]
	f_2	124.0 [N]

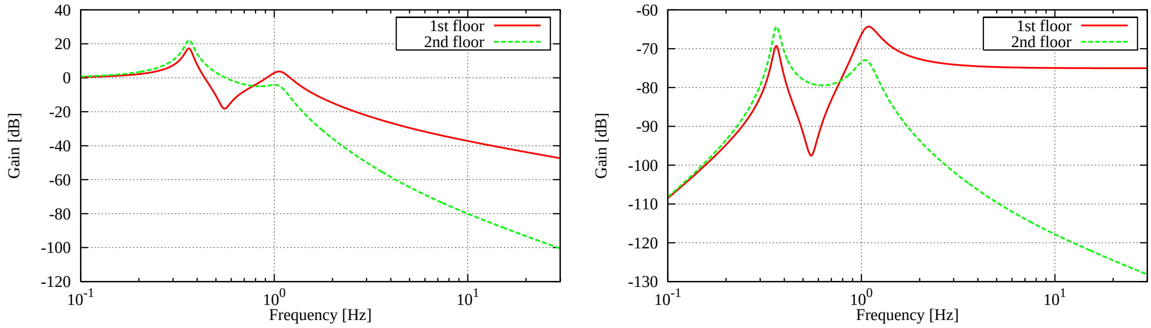

(a) From ground acceleration $\ddot{z}$ **(b) From damping force $u = c_v\,\dot{x}_1$**

Figure 2. Frequency Responses of Model

MR Damper Device

Mechanism

The MR damper is manufactured by Sanwa Tekki Corporation and contains a MR fluid developed by Bando Chemical Industries Ltd. The principle of this MR damper is simple and similar to oil damper. See Figure 3. The damper has a piston and a cylinder filled with MR fluid. The flow of the MR fluid generated by piston movement should be lead into the bypass, which difference from some commercial products of MR damper devices [3], and is subjected to magnetic field formed from surrounding coils. The main reason to put the bypass outside of the piston and the cylinder is to make a circuit of electromagnet efficiently.

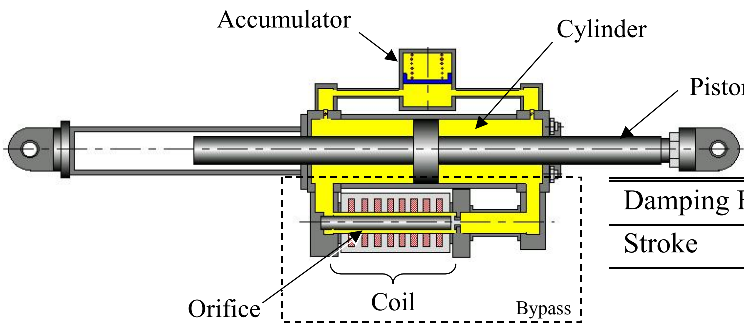

Damping Force	40	[kN]
Stroke	±295	[mm]

Figure 3. MR Damper (MRD 40kN-590)

Properties

An MR damper produces variable damping force depending on applied current and stroke velocity of piston movement. Therefore, it is very important to set up functions from input current to damping force before applying control.

On Figure 4, the solid line shows relations between stroke velocity and damping force at a certain constant current obtained from experimental test. We use the following bilinear model for the MR damper as shown by dashed line in Figure 4.

$$F = \begin{cases} \mathrm{sgn}(\dot{x}) \cdot (0.07|\dot{x}_1| + a(i)) & (|\dot{x}_1| \geq 0.1) \\ b(i)\,\dot{x}_1 & (|\dot{x}_1| < 0.1) \end{cases} \tag{1}$$

Both $a(i)$ and $b(i)$ in Eq.(1) are assumed as quadric functions about input current i. See Eq.(2) and Figure 5.

$$a(i) = \hat{a}_1\, i^2 + \hat{b}_1\, i + \hat{c}_1 \quad , \quad b(i) = \hat{a}_2\, i^2 + \hat{b}_2\, i + \hat{c}_2 \tag{2}$$

where $\hat{a}_1 = 1.5$, $\hat{b}_1 = 2.27$, $\hat{c}_1 = 0.528$, $\hat{a}_2 = 20$, $\hat{b}_2 = 20$ and $\hat{c}_2 = 5.352$.

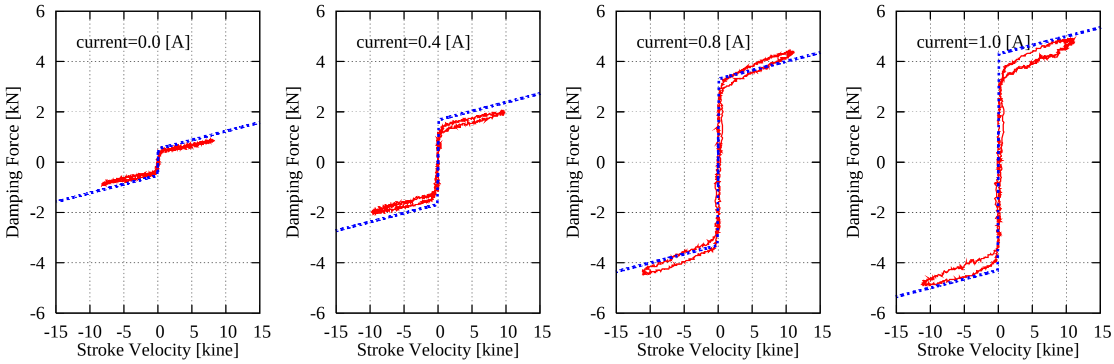

Figure 4. Characteristics of MR Damper

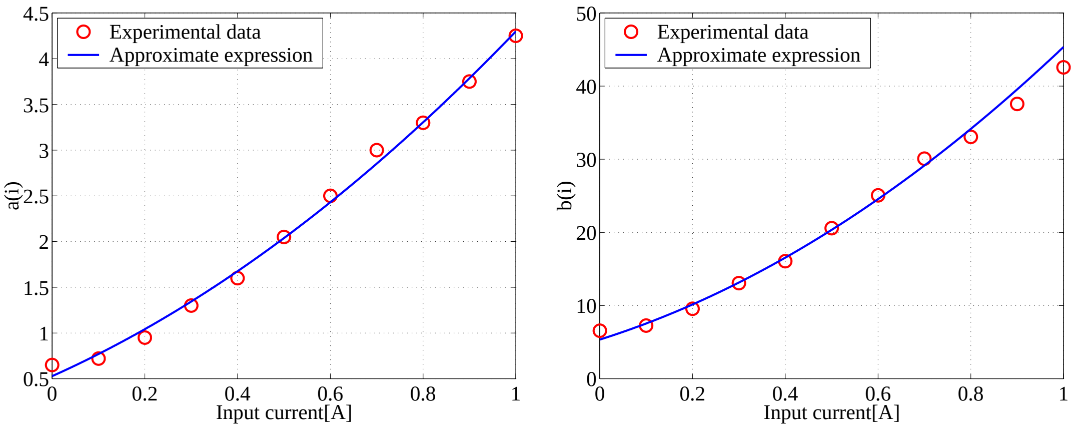

(a) $a(i)$ **(b)** $b(i)$

Figure 5. Relations between Input Current and $a(i)$, $b(i)$

CONTROL SYSTEM DESIGN

Gain-Scheduled Control Method

We apply a gain-scheduled (GS) control method to calculate an appropriate damping coefficient. The design of the GS controller is based on linear matrix inequalities (LMIs) and the controller is obtained by the convex interpolation of four-vertex linear time-invariant (LTI) controllers [4]. It is well known that the system with a semi-active damper can be modeled as a bilinear system where the input term is linear to both the damping coefficient that is regarded as the control input and the relative velocity. If linear control theory is applied to the bilinear system, switching of damping coefficient should be required frequently and the generated force is not smooth. By assuming a semi-active damper model with a controllable valve the system can be described as a linear parameter-varying (LPV) model. The LTI controller according to the vertexes can be obtained by applying LMIs and the GS controller is obtained by convex interpolation of the LTI controllers. In this paper we take two varying parameters p_1 of the stroke velocity and p_2 of the damping coefficient restriction. In order to prevent the uncontrollability caused when the stroke velocity is equal to zero, the parameter varying range is divided into two areas around small value of the velocity. See Figure 6. If parameter p_1 is in the range from –0.005 to 0.005, we make the input e zero.

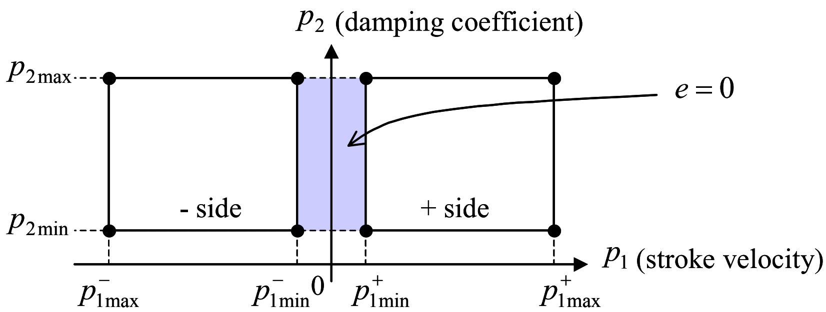

Figure 6. Separation of Parameter-varying Range

Weighting Functions

We apply the H-infinity norm criterion for each vertex. The schematic diagram of generalized plant is shown in Figure 7. While the weighting function W_T is defined not to increase the effect of control force in higher frequency, W_{S1} and W_{S2} cover the first and second mode of the controlled object respectively for reduction of the acceleration response. See Figure 8. W_T, W_{S1} and W_{S2} are given by Eqs.(3), (4) and (5) respectively. Figure 9 shows the gain of frequency response functions of the controllers at each vertex.

$$W_T = 0.52 \times \frac{s^2 + 2 \cdot 0.8 \cdot (20 \cdot 2\pi) \cdot s + (20 \cdot 2\pi)^2}{s^2 + 2 \cdot 0.4 \cdot (500 \cdot 2\pi) \cdot s + (500 \cdot 2\pi)^2} \tag{3}$$

$$W_{S1} = (8.0 \cdot 2\pi)^{12} \cdot 2.7 \cdot 10^{-14} \times \frac{s^2 + 2 \cdot 0.5 \cdot (0.8 \cdot 2\pi) \cdot s + (0.8 \cdot 2\pi)^2}{s^2 + 2 \cdot 0.5 \cdot (1.0 \cdot 2\pi) \cdot s + (1.0 \cdot 2\pi)^2} \times \frac{1}{(s^2 + 2 \cdot 0.63 \cdot (8.0 \cdot 2\pi) \cdot s + (8.0 \cdot 2\pi)^2)^2} \tag{4}$$

$$W_{S2} = (0.4 \cdot 2\pi)^8 \cdot 0.14^2 \times \frac{1}{(s^2 + 2 \cdot 0.5 \cdot (0.4 \cdot 2\pi) \cdot s + (0.4 \cdot 2\pi)^2)^2} \tag{5}$$

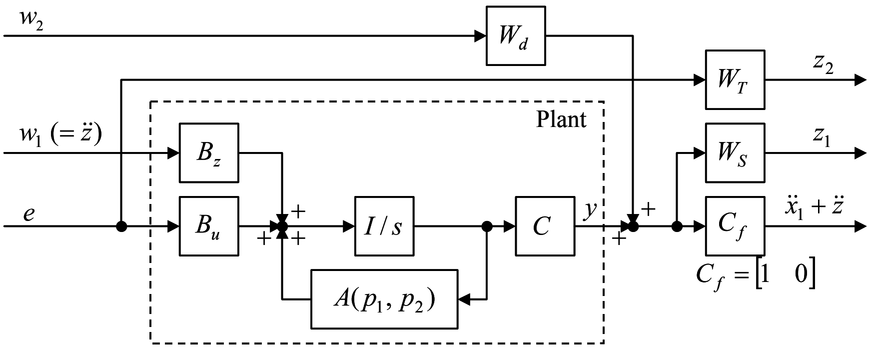

Figure 7. Generalized Plant

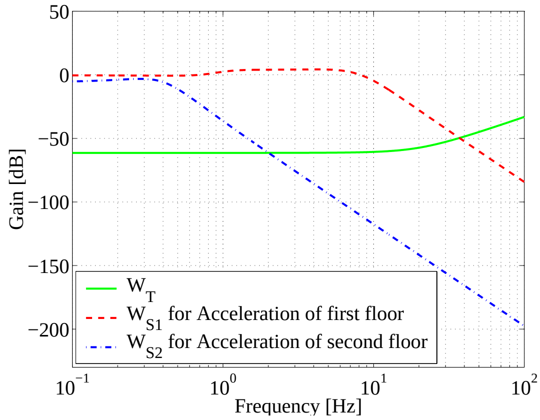

Figure 8. Frequency Responses of Weighting Functions

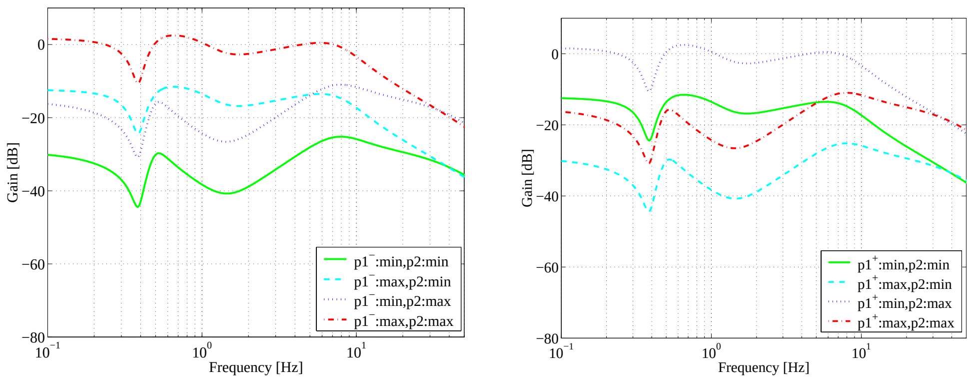

(a) Negative side **(b) Positive side**

Figure 9. Frequency Responses of Vertex Controllers

RESULT

SHAKING TABLE TEST

In this section, the performance of the GS controller is compared to the other result of the passive systems with constant damping coefficient 42500 Ns/m, 7000 Ns/m and 24750 Ns/m (mean of former two values) which are referred to as hard, soft and medium damping respectively.

Figure 10 shows the frequency response of mass acceleration to ground acceleration with the MR damper. From Figure 10, we can see that not only the first and second modes are suppressed but also the response in higher frequency range than the second mode is suppressed more than a medium damper.

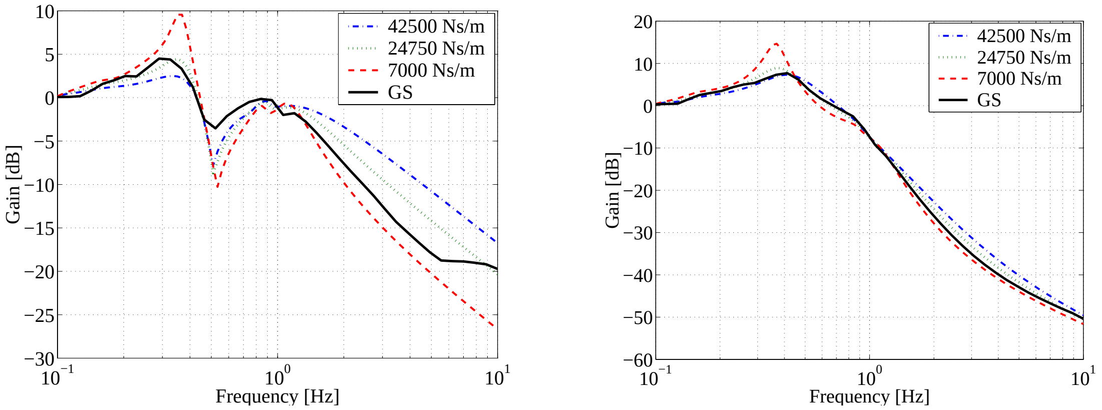

(a) First floor **(b) Second floor**

Figure 10. Frequency Responses of Mass Acceleration to Ground Acceleration

Figure 11 shows the comparison of experimental and simulation results for GS control under Hachinohe 1968NS earthquake normalized as 25kine of maximum velocity. The structural responses of simulation results show good agreement with those of experimental ones. However, some errors can be seen on hysteresis of MR damper forces (Figure 11(b)). There are some possible reasons for this, such as mechanical gaps, unconsidered behavior in high stroke velocity, etc.

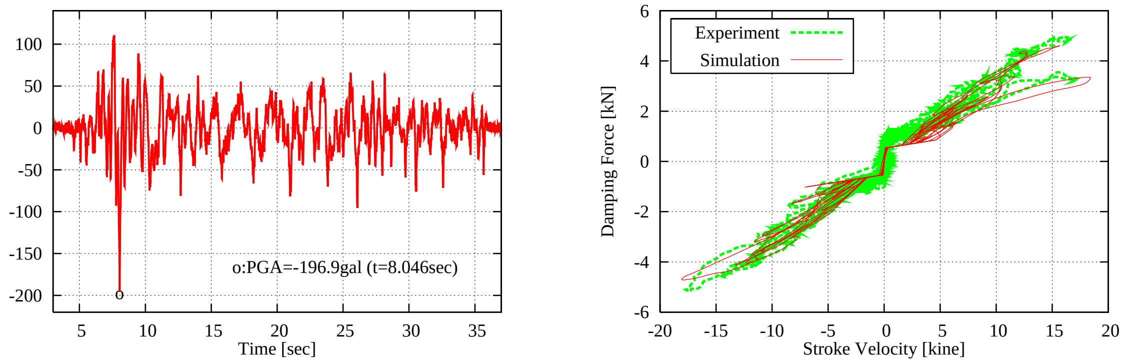

(a) Hachinohe 1968NS earthquake **(b) Stroke velocity and damping force**

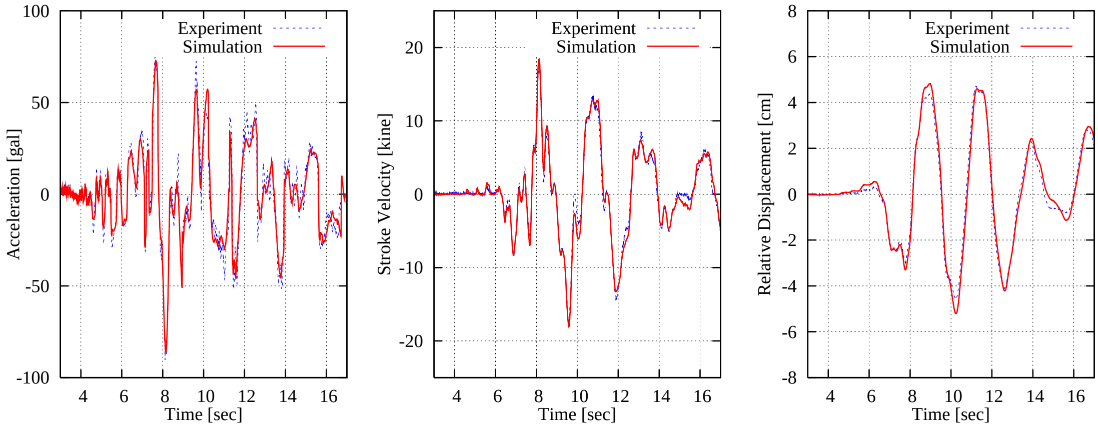

(c) Time history of first floor

Figure 11. Comparison of Experimental and Numerical Results

Figure 12 shows the experimental result of the GS control in comparison with the passive systems. From Figures 12(b) and 12(c), it can be seen that at the time before 7.5 sec the GS controller makes the damping coefficient c_v small like a soft damper and the acceleration response are suppressed. At the time after 7.5 sec the damping coefficient becomes large values like a hard damper. The GS controller can output the appropriate damping coefficient. From viewpoint of acceleration response of the first floor, the medium passive damper seems to have better performance but the GS control can suppress both acceleration and displacement at the same time. See Figure 13.

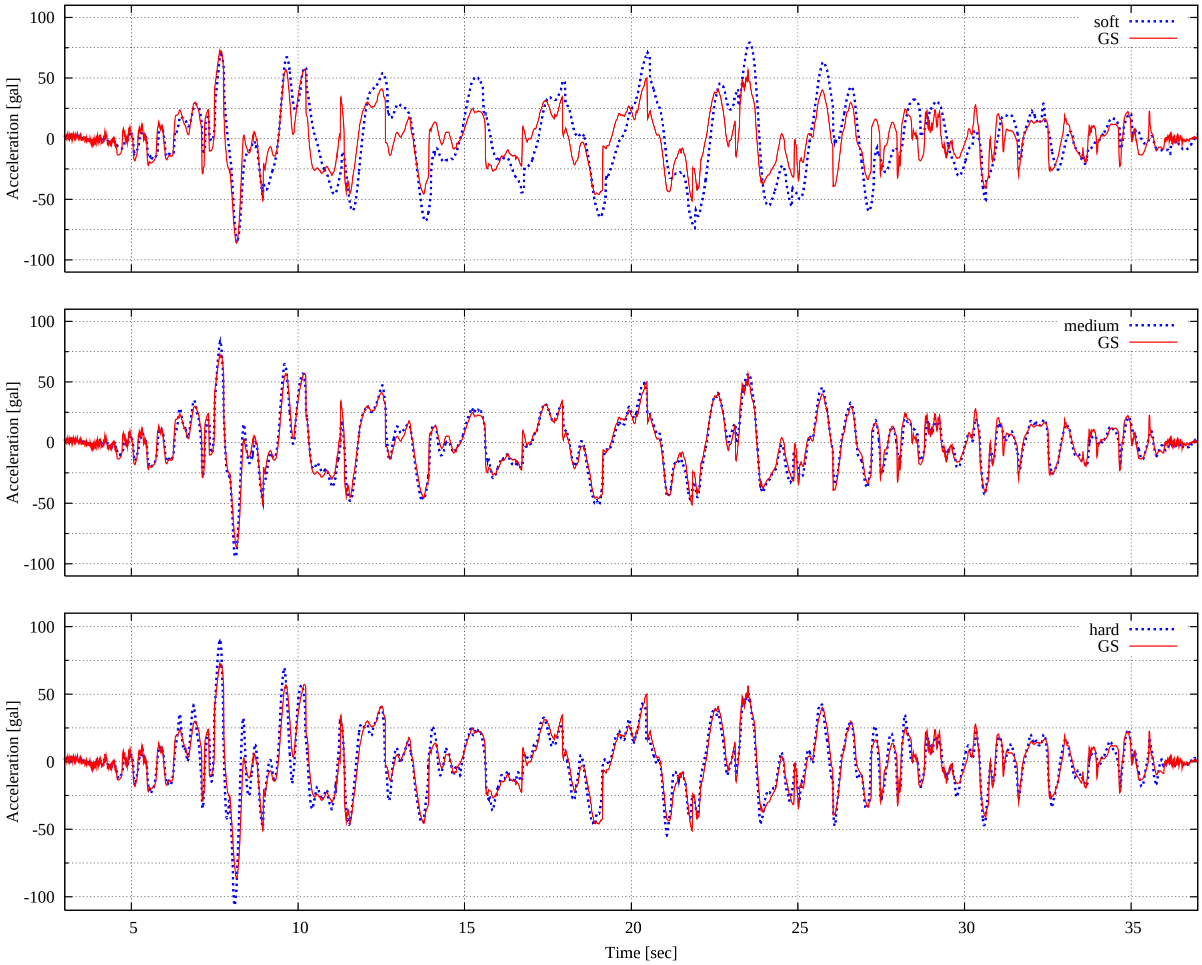

(a) Acceleration of first floor

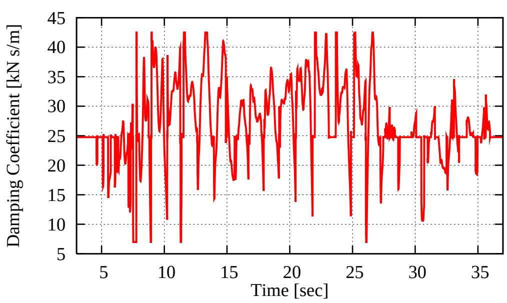

(b) Damping coefficient c_v

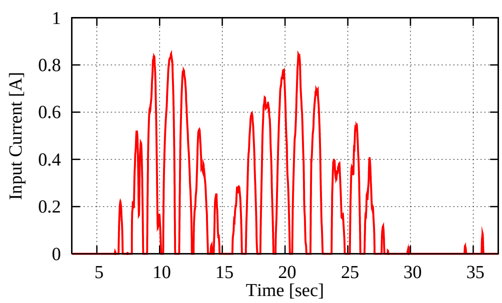

(c) Input current

Figure 12. Time History of Response

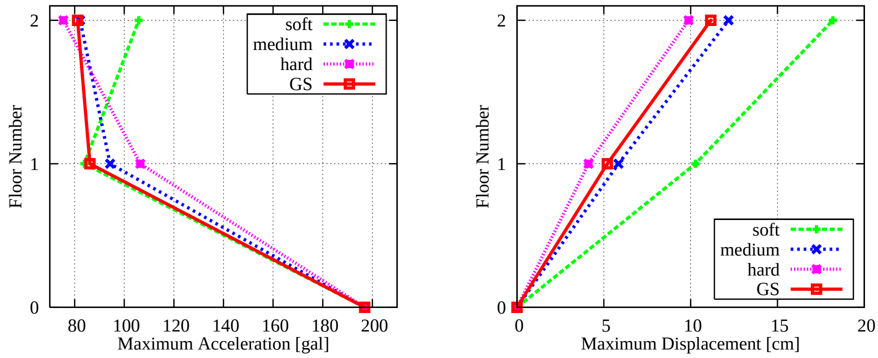

Figure 13. Maximum Amplitude of Each Floor against Hachinohe Earthquake

PERFORMANCE

To discuss about structural design, it is important to consider not only the time history but also the total input energy to the upper structure. Since it is said that the total input energy for structure can be associated with the velocity response spectrum of ground motion [5], then, the performance of control may compared by using response spectra of acceleration response observed at first floor. Figure 14 shows the velocity response spectrum ratio r about passive systems under various earthquakes normalized as 25kine (Figure 14(a)) and 50kine (Figure 14(b)). The horizontal line r=1.0 on these figures means the reference, i.e. the velocity response spectrum (h=5%) of the GS controller using acceleration response of first floor. It can be said that the GS control shows good performance in the right half of plotted area. In lower period the soft passive system can suppress the response better than the GS control but it has excessive peak around 2.8sec, the first mode of isolated system.

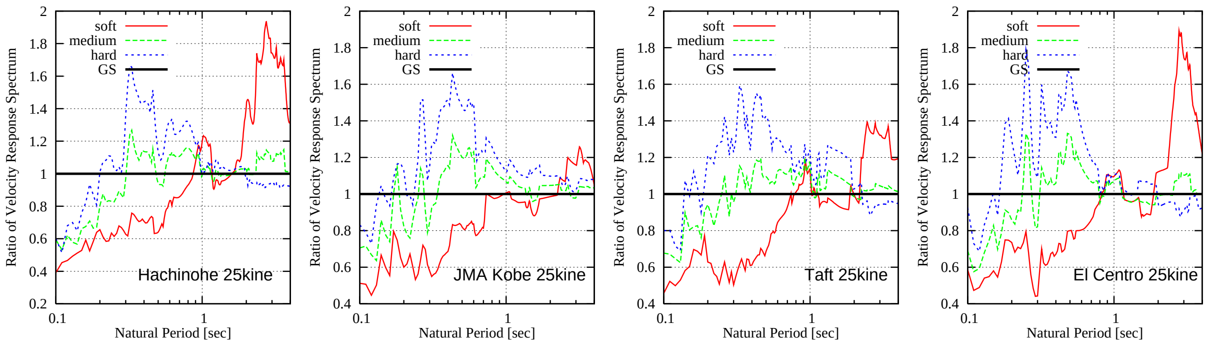

(a) For 25kine

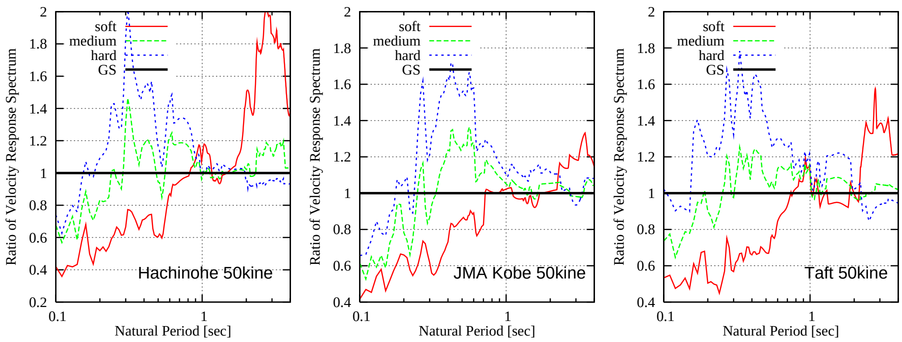

(b) For 50kine

Figure 14. Ratio of Velocity Response Spectrum (h=5%)

Figure 15 shows the average of the ratio of velocity response spectrum around the first and second mode of isolated system. This also shows the same pattern mentioned above. In these figures, four waves (Hachinohe, JMA Kobe, Taft and El Centro) of 25kine and three (Hachinohe, JMA Kobe and Taft) of 50kine in order from left to right, are plotted together. The soft damping system has good performance in lower period ($0.1 < T < 2.0$) but got worse in higher period ($2.0 \leq T < 4.0$). Performance of the hard damping system is contrary to that of the soft damping system. Compared to the average for overall range plotted in Figure 14, none of average values have been less than 1.0. This means that the GS control shows the best performance.

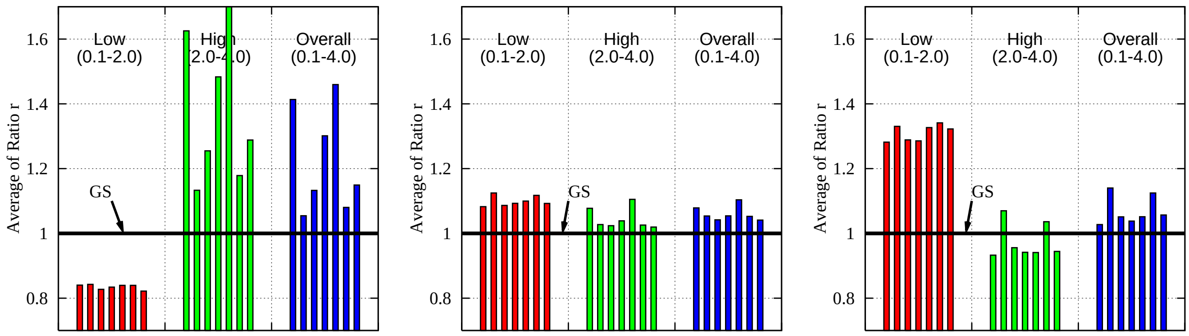

(a) Soft damping **(b) Medium damping** **(c) Hard damping**

Figure 15. Input Reduction for Earthquakes

CONCLUSIONS

A shaking table test and a numerical analysis has been carried out to confirm the efficiency of the semi-active MR damper device for the response control of the base isolated structure. The structural system with the MR damper was modeled as a linear parameter-varying system properly and it was verified that the GS control applied in this study provides higher performance in comparison with the passive control. The dynamic model of the MR damper device could be traced well all along the shaking table test.

ACKNOWLEDGEMENT

A part of this study was financially supported by the Budget for Nuclear Research of the Ministry of Education, Culture, Sports, Science and Technology, based on the screening and counseling by the Atomic Energy Commission.

This research work has been carried out under the Smart Material working group organized in the cooperative research project on a base isolation and vibration control for building structures. The authors wish to thank the members from Kumagaigumi Co., Ltd., Satokogyo Co., Ltd., Toda Corporation, Nishimatsu Construction Co., Ltd., Hazama Corporation, Fujita Corporation and Maeda Corporation for their fruitful discussions.

This research work was partly supported by the project on a technology to translate the Smart Structural Systems into practical applications, held in Building Research Institute (BRI). The shaking table test was conducted with the cooperation of Mr. Hisaaki IMAZATO, Cooperative researcher of BRI. His cooperation is gratefully acknowledged.

REFERENCES

1. Soda, S., Kusumoto, H., Chatani, R., Iwata, N., Fujitani, H., Shiozaki, Y. and Hiwatashi, T. "Semi-active Seismic Response Control of Base-isolated Building with MR Damper", Proceedings of the SPIE's 10^{th} Annual International Symposium on Smart Structures and Materials, No.5052-56, 2003.
2. Hiwatashi, T., Shiozaki, Y., Minowa, C. and Soda, S. "Shaking Table Tests on Semi-active Base-isolation System by Magnetorheological Fluid Damper", Proceedings of the SPIE's 10^{th} Annual International Symposium on Smart Structures and Materials, No.5056-50, 2003.
3. http://www.lord.com/
4. Nishimura, H., Okumura, Y. and Shimodaira, S. "Semi-active Vibration Isolation Control for Multi-degree-of-freedom Structures", Proc. of 2002 ASME PRESSURE VESSELS & PIPING CONFERENCE, Vol. 445-2, pp.189-196, 2002.
5. Akiyama, H. "Earthquake-Resistant Design Method for Buildings Based on Energy Balance", Gihodo Shuppan Co. Ltd., 1999 (in Japanese).